



# Group 1 innate lymphoid cells are involved in the progression of experimental anti-glomerular basement membrane glomerulonephritis and are regulated by peroxisome proliferator-activated receptor $\alpha$

Yusuke Okabayashi<sup>1,2</sup>, Shinya Nagasaka<sup>1</sup>, Go Kanzaki<sup>2</sup>, Nobuo Tsuboi<sup>2</sup>, Takashi Yokoo<sup>2</sup> and Akira Shimizu<sup>1</sup>

<sup>1</sup>Department of Analytic Human Pathology, Nippon Medical School, Tokyo, Japan; and <sup>2</sup>Division of Nephrology and Hypertension, Department of Internal Medicine, The Jikei University School of Medicine, Tokyo, Japan

Innate lymphoid cells play an important role in the early effector cytokine-mediated response. In Wistar Kyoto rats, CD8<sup>+</sup> non-T lymphocytes (CD8<sup>+</sup>Lym) infiltrate into glomeruli during the development of anti-glomerular basement membrane (anti-GBM) glomerulonephritis. Here, we examined the profiles and roles of CD8<sup>+</sup>Lym in anti-GBM glomerulonephritis. The regulation of CD8<sup>+</sup>Lym by peroxisome proliferator-activated receptor (PPAR)- $\alpha$  in anti-GBM glomerulonephritis was also evaluated. Glomerular infiltrating CD8<sup>+</sup>Lym were lineage-negative cells that showed markedly high expression of *IFN- $\gamma$*  and *T-bet* mRNAs but not *Eomes*, indicating these cells are group 1 innate lymphoid cells. In anti-GBM glomerulonephritis, the glomerular mRNAs of innate lymphoid cell-related cytokines (*IFN- $\gamma$*  and *TNF- $\alpha$* ) and chemokines (*CXCL9*, *CXCL10*, and *CXCL11*) are significantly increased. Treatment with a PPAR $\alpha$  agonist ameliorated renal injury, with reduced expression of these mRNAs. *In vitro*, enhanced IFN- $\gamma$  production from innate lymphoid cells upon IL-12 and IL-18 stimulation was reduced by the PPAR $\alpha$  agonist. Moreover, *CXCL9* mRNA in glomerular endothelial cells and *CXCL9*, *CXCL10*, and *CXCL11* mRNAs in podocytes and macrophages were upregulated by IFN- $\gamma$ , whereas the PPAR $\alpha$  agonist downregulated their expression. We also detected the infiltration of innate lymphoid cells into glomeruli in human anti-GBM glomerulonephritis. Thus, innate lymphoid cells are involved in the progression of anti-GBM glomerulonephritis and regulated directly or indirectly by PPAR $\alpha$ . Our findings suggest that innate lymphoid cells could serve as novel therapeutic targets for anti-GBM glomerulonephritis.

*Kidney International* (2019) **96**, 942–956; <https://doi.org/10.1016/j.kint.2019.04.039>

KEYWORDS: chemokine; crescentic GN; IFN- $\gamma$ ; ILC1; PPAR

Copyright © 2019, International Society of Nephrology. Published by Elsevier Inc. All rights reserved.

**Correspondence:** Akira Shimizu, Department of Analytic Human Pathology, Nippon Medical School, 1-1-5, Sendagi, Bunkyo-ku, Tokyo 113-8602, Japan. E-mail: [ashimizu@nms.ac.jp](mailto:ashimizu@nms.ac.jp)

Received 5 November 2018; revised 23 April 2019; accepted 25 April 2019; published online 22 May 2019

## Translational Statement

Recently identified innate lymphoid cells (ILC1s) regulate early immune responses as innate immune cells prior to the development of adaptive immunity; they also exhibit phenotypic and functional characteristics that resemble those of T helper cell 1 cells. The present study revealed the involvement of ILC1s in the progression of experimental rat anti-glomerular basement membrane glomerulonephritis and the direct and indirect effects of a proliferator-activated receptor- $\alpha$  agonist on ILC1 regulation. Furthermore, in human anti-glomerular basement membrane glomerulonephritis, ILC1s were detected in glomeruli, particularly prior to the development of crescent formation, suggesting that ILC1s are involved in the early phase of inflammation. These results constitute evidence that ILC1s could serve as a novel therapeutic target; moreover, based on their ability to regulate ILC1s, proliferator-activated receptor- $\alpha$  agonists might be a suitable treatment for patients with anti-glomerular basement membrane glomerulonephritis.

Innate lymphoid cells (ILCs) are a novel group of immune cells. ILCs are classified into group 1, 2, and 3 ILCs based on their phenotypic and functional characteristics of T helper cell 1 (Th1), Th2, and Th17 cells, respectively. Hence, ILC1s, including natural killer (NK) cells, are characterized by the production of interferon- $\gamma$  (IFN- $\gamma$ ) and the expression of transcription factor T-box factor expressed in T cells (T-bet). However, unlike T and B cells, ILCs do not express adaptive antigen recognition receptors or phenotypic markers of myeloid or dendritic cells. Instead, their functions are mediated by cytokine signals from myeloid and non-hematopoietic cells.<sup>1–3</sup> ILC1s regulate early immune responses against the type of encountered pathogen or tissue damage, and their migration is regulated by chemokine ligand 9 (CXCL9), CXCL10, and CXCL11, because ILC1s express CXC chemokine receptor 3, which is activated by the above-mentioned chemokines.<sup>4</sup> High proportions of ILC1s have been found in patients with several diseases, suggesting an association between ILC1s and the pathogenesis of inflammatory diseases.<sup>5–8</sup>

In a rat model of anti-glomerular basement membrane (anti-GBM) glomerulonephritis (GN), crescentic GN develops with infiltration of CD8<sup>+</sup>Lym and activated macrophages (M $\phi$ ).<sup>9–14</sup> During adaptive immunity, infiltrating M $\phi$  regulated by T helper cell subsets (Th1, Th2, and Th17 cells) directly induced glomerular injury, including crescent formation.<sup>15–19</sup> Experimental anti-GBM GN is attenuated by inhibiting the function of or changing the phenotype of M $\phi$ .<sup>9,10</sup> In rat models of anti-GBM GN, CD8<sup>+</sup>Lym infiltrate into glomeruli from an early phase of inflammation, and the depletion of CD8<sup>+</sup>Lym markedly reduces the amount of M $\phi$  infiltration into glomeruli, resulting in an improvement of crescentic GN with the suppression of glomerular IFN- $\gamma$  expression.<sup>11,12</sup> In contrast, migration inhibition of M $\phi$  have no effect on the number of CD8<sup>+</sup>Lym that infiltrate into glomeruli, despite improvements in anti-GBM GN.<sup>13</sup> These results indicate that glomerular injury directly induced by M $\phi$  is regulated by CD8<sup>+</sup>Lym. However, little is known regarding the profile of CD8<sup>+</sup>Lym in the development of anti-GBM GN.

PPAR $\alpha$  belongs to the nuclear receptor family of ligand-activated transcription factors that regulates gene expression involved in lipid metabolism, atherosclerosis, neo-vascularization, and inflammation.<sup>20–22</sup> PPAR $\alpha$  is expressed in various tissues and cells, including the kidney, lymphocytes, and M $\phi$ .<sup>22,23</sup> Therefore, in rodent models of inflammatory and autoimmune diseases, PPAR $\alpha$  signaling is widely used to regulate immune responses.<sup>21,24–31</sup> Although several studies have been published on the anti-inflammatory effect of PPAR $\alpha$  via the regulation of inflammatory cytokines and chemokines, only a few have focused on the effects and mechanism of action of PPAR $\alpha$  on the regulation of cytokines and chemokines in anti-GBM GN.<sup>24–27</sup>

In this study, we investigated the profiles and roles of glomerular-infiltrating CD8<sup>+</sup>Lym and the therapeutic effects of PPAR $\alpha$  on the regulation of CD8<sup>+</sup>Lym in the development of anti-GBM GN in Wistar Kyoto rats.

## RESULTS

### Identification of the CD8<sup>+</sup>Lym profile

Severe necrotizing and crescentic GN was induced by a single injection of anti-rat GBM antibody (Figure 1a). As previously reported, a large number of M $\phi$  and CD8<sup>+</sup>Lym infiltrated into glomeruli on day 7 (Figure 1b and c).<sup>9,10,32</sup> Immunofluorescence microscopy showed that most of the glomerular-infiltrating CD8<sup>+</sup>Lym did not express CD3, CD68, CD103, or CD161 (Figure 1d and e, Supplementary Table S1A). Similarly, flow cytometric analysis revealed that the majority of the glomerular-infiltrating CD8<sup>+</sup> cells were lineage marker (CD3, CD4, CD14, CD45R, CD103, CD161, and granulocyte marker)-negative (Lin<sup>−</sup>) (Figure 1f and g, Supplementary Table S1B and C); nearly all of the glomerular-infiltrating Lin<sup>−</sup> cells expressed CD8 (Supplementary Figure S1, Supplementary Table S1D). Approximately 5% to 10% of leukocytes that infiltrated into glomeruli were CD8<sup>+</sup>Lym. To identify the functional characteristics of CD8<sup>+</sup>Lym, we further examined the mRNA expression of CD8<sup>+</sup>Lym.

Quantitative real-time polymerase chain reaction (qRT-PCR) analysis revealed that IFN- $\gamma$  and *T-bet* mRNAs were markedly high in CD8<sup>+</sup>Lym, compared with M $\phi$ . The expression of *tumor necrosis factor- $\alpha$*  (*TNF- $\alpha$* ) mRNA in CD8<sup>+</sup>Lym was not different from that in M $\phi$  (Figure 1h, Supplementary Table S1E). Moreover, CD8<sup>+</sup>Lym displayed significantly lower levels of *eomesodermin* (*Eomes*) mRNA, compared with conventional NK cells (Lin<sup>−</sup>CD161<sup>+</sup> cells) (Supplementary Figure S2A and B, Supplementary Table S1F). To detect the major source of IFN- $\gamma$  in the early phase of anti-GBM GN, we next investigated the IFN- $\gamma$ -producing cells in glomeruli. Flow cytometric analysis revealed that CD8<sup>+</sup>Lym comprised the majority of cells expressing IFN- $\gamma$  in the early phase of anti-GBM GN (Figure 1i and j). These data indicate that the phenotype of glomerular-infiltrating CD8<sup>+</sup>Lym is identical to that of ILC1s; moreover, CD8<sup>+</sup>Lym are the major IFN- $\gamma$ -producing cells in the early phase of anti-GBM GN.

### Glomerular ILC1-related cytokines and chemokines expression in anti-GBM GN rats

We next examined whether the glomerular expression of ILC1-related genes was upregulated in anti-GBM GN rats. The qRT-PCR analysis revealed that, in anti-GBM GN, there were significant increases in the glomerular expression of ILC1-related cytokines (*IFN- $\gamma$*  and *TNF- $\alpha$* ) and chemokines (*CXCL9*, *CXCL10*, and *CXCL11*) (Figure 2a and b, Supplementary Table S1G), as well as that of *interleukin (IL)-1 $\beta$* , *inducible nitric oxide synthase (iNOS)*, and *C-C motif chemokine ligand 2 (CCL2)*, all of which are associated with M $\phi$  (Figure 2c, Supplementary Table S1G). Likewise, the ILC1-related transcription factor *T-bet*, and *IL-12p40*, which activate ILC1, were significantly upregulated (Figure 2a and d, Supplementary Table S1G). However, the expression of *IL-18* mRNA, which is associated with the activation of immune cells, including ILC1 and Th1 cells, was not upregulated in anti-GBM GN (data not shown).

### PPAR $\alpha$ activation attenuated anti-GBM GN

Because PPAR $\alpha$  agonists regulate inflammatory cytokines and chemokines, including IFN- $\gamma$ , *CXCL9*, *CXCL10*, and *CXCL11*, we examined the expression of PPAR $\alpha$  in anti-GBM GN.<sup>24–27</sup> Nearly all glomerular-infiltrating CD8<sup>+</sup>Lym expressed PPAR $\alpha$  (Figure 3a and b, Supplementary Table S1H); both CD8<sup>+</sup>Lym and M $\phi$  equally expressed mRNA for PPAR $\alpha$  and *enoyl-CoA hydratase and 3-hydroxyacyl CoA dehydrogenase (Ehhadh*, a target gene of PPAR $\alpha$ ) (Figure 3c, Supplementary Table S1I). On induction of anti-GBM GN, the expression levels of PPAR $\alpha$  and *Ehhadh* mRNAs were significantly downregulated (Figure 3d, Supplementary Table S1J). These results suggested that glomeruli disruption leads to downregulation of PPAR $\alpha$ ; moreover, PPAR $\alpha$  may regulate the activation of CD8<sup>+</sup>Lym and M $\phi$ . We next examined the effects of PPAR $\alpha$  on anti-GBM GN. In vehicle-treated control rats (control group), the levels of serum creatinine gradually increased in a time-dependent manner and significantly improved in anti-GBM GN rats treated with a PPAR $\alpha$  agonist (PPAR $\alpha$  group)

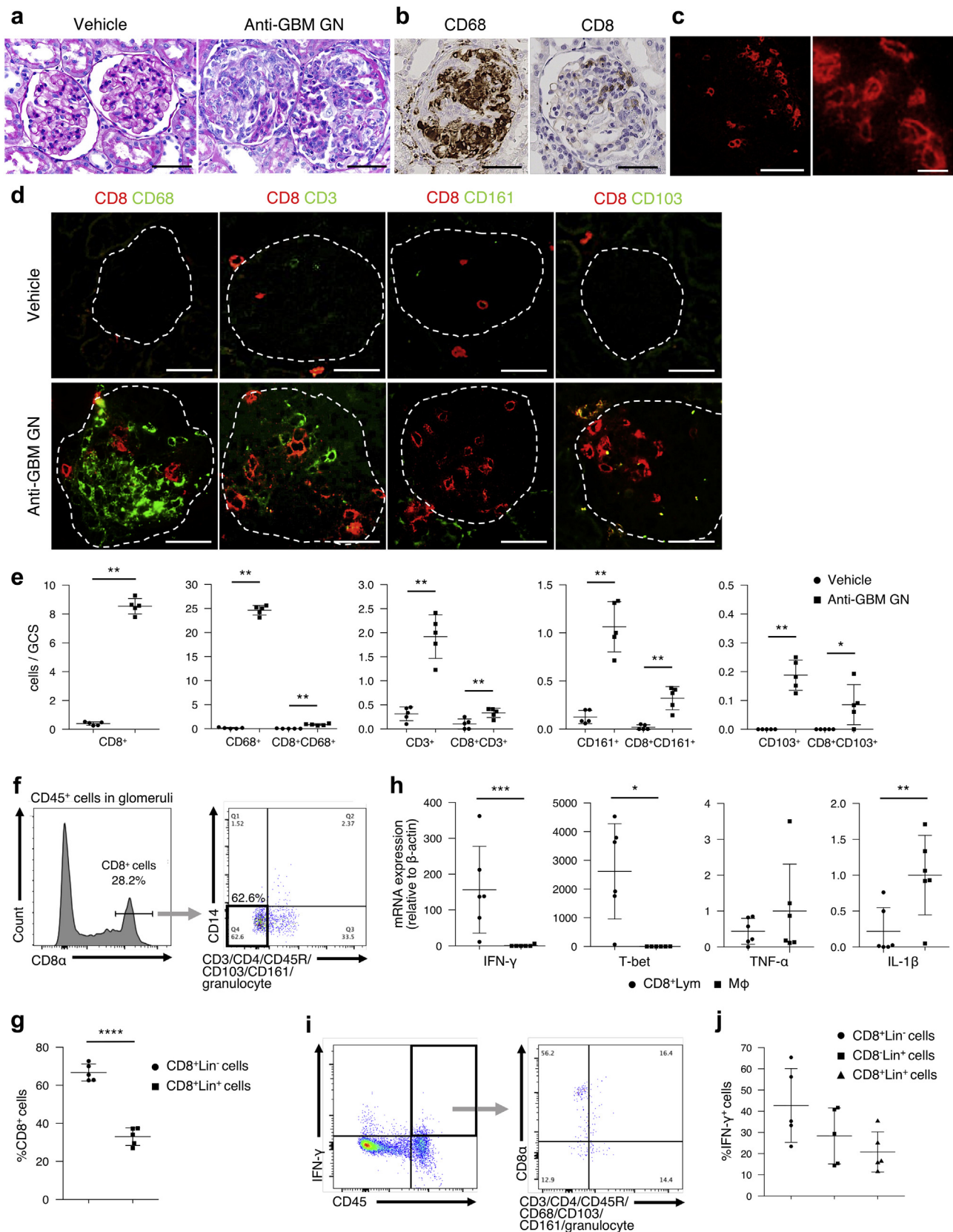


**Figure 1 | The characteristics of CD8<sup>+</sup> non-T lymphocytes (CD8<sup>+</sup>Lym) were consistent with those of group 1 innate lymphoid cells. (a) Representative light microscopic findings in vehicle and anti-glomerular basement membrane (anti-GBM) glomerulonephritis (GN) (periodic acid-Schiff stain). (b) Representative immunohistochemical staining for CD68 and CD8 in anti-GBM GN. (c) Representative immunofluorescence staining for CD8 (red) in anti-GBM GN. (d) Representative immunofluorescence staining for (continued)**

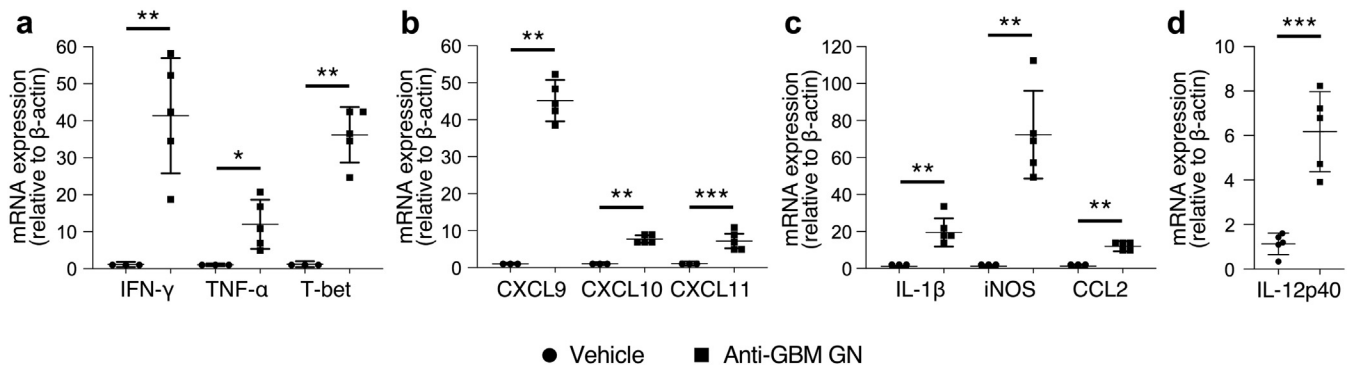


**Figure 2 | Expression of group 1 innate lymphoid cell-related cytokine and chemokine mRNAs was significantly upregulated in the glomeruli of anti-glomerular basement membrane (anti-GBM) glomerulonephritis (GN) rats.** Quantitative real-time polymerase chain reaction analysis of mRNAs for group 1 innate lymphoid cell-related cytokines and transcription factors, including *interferon- $\gamma$*  (IFN- $\gamma$ ), *tumor necrosis factor- $\alpha$*  (TNF- $\alpha$ ), and *T-box factor expressed in T cells* (T-bet) (a); group 1 innate lymphoid cell-related chemokines, including *CXC chemokine ligand 9* (CXCL9), CXCL10, and CXCL11 (b); macrophage-related genes, including *interleukin-1  $\beta$*  (IL-1 $\beta$ ), *inducible nitric oxide synthase* (iNOS), and *C-C motif chemokine ligand 2* (CCL2) (c); and *IL-12p40* (d), in isolated glomeruli. Results are normalized to  $\beta$ -actin and are presented as relative expression compared with that of the vehicle group (set as 1). Values represent the mean  $\pm$  SD of evaluations from each group ( $n = 5$  per group). \* $P < 0.05$ , \*\* $P < 0.01$ , and \*\*\* $P < 0.005$ .

(Figure 3e, Supplementary Table S1K). The large amount of albuminuria detected in control group on day 7 showed a decreasing trend in the PPAR $\alpha$  group (Figure 3f, Supplementary Table S1K). Similarly, necrotizing and crescentic glomeruli were significantly reduced in the PPAR $\alpha$  group on day 7 (Figure 3g and h, Supplementary Table S1K). In the control group, the number of glomerular-infiltrating CD68 $^{+}$  M $\phi$  gradually increased from days 3 to 7 (Figure 3i and l, Supplementary Table S1K). In contrast, the number of glomerular-infiltrating CD8 $^{+}$ Lym markedly increased from days 5 to 7 (Figure 3j and m, Supplementary Table S1K). On days 3 and 5, very few CD3 $^{+}$  T cells were detected in glomeruli (Figure 3k and n, Supplementary Table S1K). By day 7, the number of glomerular-infiltrating CD3 $^{+}$  T cells had slightly increased. Administration of the PPAR $\alpha$  agonist significantly reduced the glomerular infiltration of M $\phi$ , CD8 $^{+}$  Lym, and CD3 $^{+}$  T cells on day 7 (Figure 3i–n, Supplementary Table S1K).

#### PPAR $\alpha$ signaling suppressed glomerular expression of ILC1-related cytokines and chemokines *in vivo*

To elucidate the mechanism of PPAR $\alpha$  agonist activity in anti-GBM GN, we next examined the glomerular cytokine and

chemokine environment. The qRT-PCR analysis revealed that the glomerular mRNAs of ILC1-related cytokines and chemokines were significantly suppressed on days 5 and 7 in the PPAR $\alpha$  group (Figure 4a, b, and d–f; Supplementary Table S1L); however, the PPAR $\alpha$  agonist caused no reductions in either the number of glomerular-infiltrating CD8 $^{+}$ Lym or the expression of *T-bet* mRNA on day 5 (Figures 3f and h and 4c, Supplementary Table S1K and L). The expression of *IL-12p40* mRNA was not downregulated by administration of the PPAR $\alpha$  agonist (Figure 4j, Supplementary Table S1L). These findings suggest that the PPAR $\alpha$  agonist inhibited ILC1 accumulation into glomeruli and directly suppressed ILC1 activation. Treatment with the PPAR $\alpha$  agonist also significantly decreased the expression of M $\phi$ -related cytokine and chemokine mRNAs (Figure 4g–i, Supplementary Table S1L). In contrast, upregulation of the mRNAs for *intercellular adhesion molecule-1* (ICAM-1) and *vascular cell adhesion molecule-1* (VCAM-1), which are mainly expressed on glomerular endothelial cells (GEnCs), *Eomes*, and *T-cell receptor  $\beta$* , which is mainly expressed on T cells and NK T cells, was not suppressed in the PPAR $\alpha$  group (Figure 4k and l, Supplementary Figure S3A, and Supplementary Table S1L and M). Downregulation of the

**Figure 1 |** (continued) CD8 (red), CD68 (green), CD3 (green), CD161 (green), and CD103 (green) in vehicle and anti-GBM GN. Original magnification  $\times 400$  (a, b, c [left], d) and  $\times 600$  (c [right]). (e) Numbers of glomerular-infiltrating single- and dual-stained cells were counted in vehicle or anti-GBM GN groups. Cell infiltration was quantified by the mean numbers of single- and dual-stained cells per glomerulus in 30 glomerular cross sections (GCSs), respectively. (f) Representative flow cytometric analyses of glomeruli isolated from Wistar Kyoto rats on day 7 following the induction of anti-GBM GN. The left panel shows the expression of CD8 $\alpha$  on CD45 $^{+}$  glomerular-infiltrating leukocytes. CD8 $\alpha^{+}$  lineage marker (Lin) $^{-}$  (CD3 $^{-}$ CD4 $^{-}$ CD14 $^{-}$ CD45R $^{-}$ CD103 $^{-}$ CD161 $^{-}$ granulocyte $^{-}$ ) glomerular-infiltrating leukocytes are shown in the right panel (black outlined area). (g) Frequencies of CD8 $^{+}$ Lin $^{-}$  cells and CD8 $^{+}$ Lin $^{+}$  cells in glomerular-infiltrating CD8 $^{+}$  cells. (h) Quantitative real-time polymerase chain reaction analysis of mRNA for *interferon- $\gamma$*  (IFN- $\gamma$ ), *T-box factor expressed in T cells* (T-bet), *tumor necrosis factor- $\alpha$*  (TNF- $\alpha$ ), and *interleukin-1  $\beta$*  (IL-1 $\beta$ ) in isolated glomerular-infiltrating CD8 $^{+}$ Lym and macrophages (M $\phi$ ), defined as CD8 $^{+}$ Lin $^{-}$  cells and CD14 $^{+}$  cells, respectively. Results are normalized to  $\beta$ -actin and are presented as relative expression compared with that of M $\phi$  (set as 1). (i) Representation of IFN- $\gamma$  expression in isolated glomeruli obtained from anti-GBM GN rats. (j) Frequencies of CD8 $^{+}$ Lin $^{-}$  cells, CD8 $^{+}$ Lin $^{+}$  cells, and CD8 $^{+}$ Lin $^{+}$  cells in glomerular-infiltrating CD45 $^{+}$ IFN- $\gamma^{+}$  cells. Values represent the mean  $\pm$  SD of evaluations from each group (e, g, i:  $n = 5$  per group; h:  $n = 6$  per group). \* $P < 0.05$ , \*\* $P < 0.01$ , \*\*\* $P < 0.005$ , and \*\*\*\* $P < 0.001$ . To optimize viewing of this image, please see the online version of this article at [www.kidney-international.org](http://www.kidney-international.org).

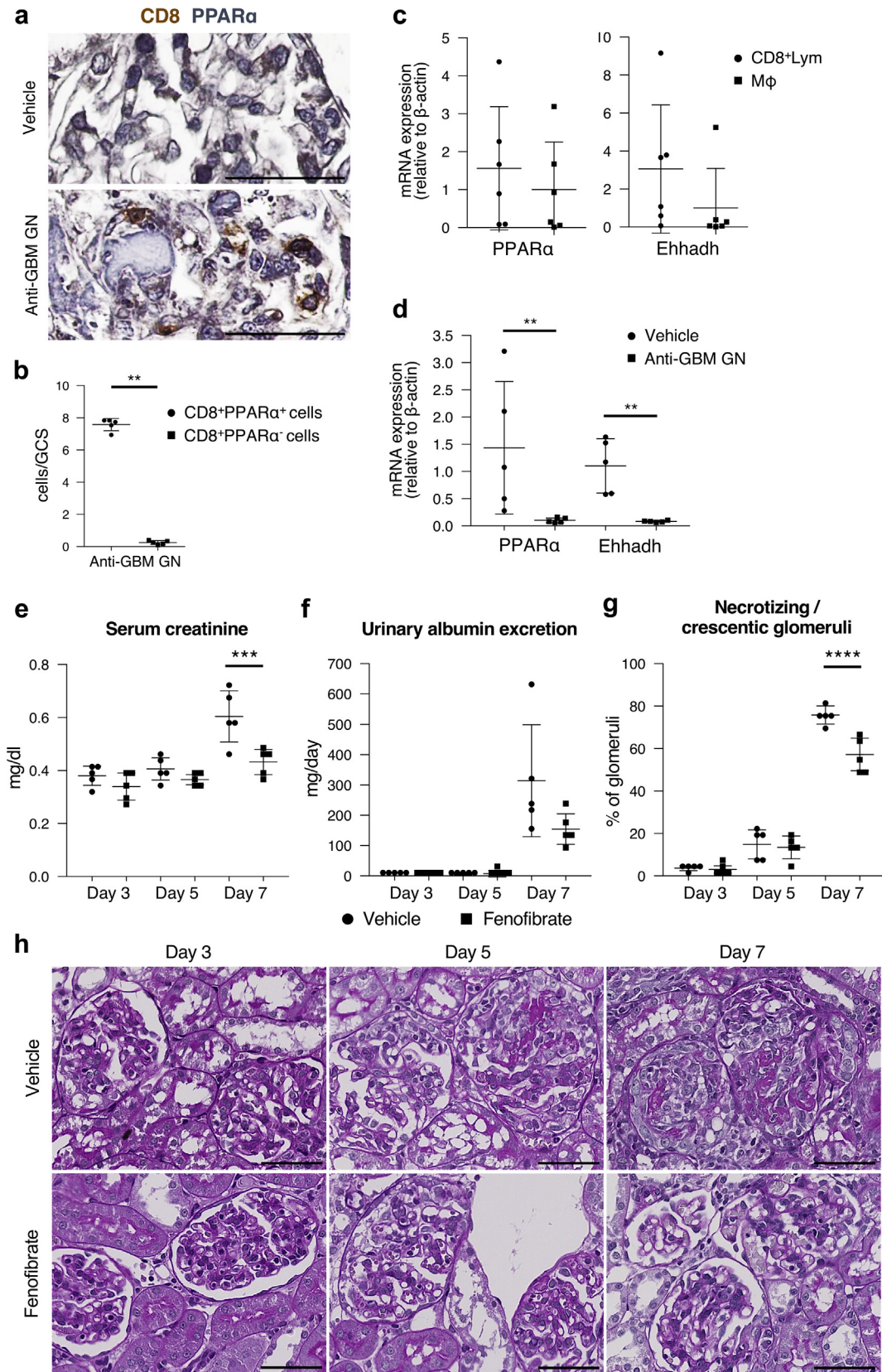


**Figure 3 | Peroxisome proliferator-activated receptor- $\alpha$  (PPAR $\alpha$ ) activation attenuated glomerular injury in anti-glomerular basement membrane (anti-GBM) glomerulonephritis (GN) by inhibiting group 1 innate lymphoid cells and macrophage (M $\phi$ ) migration into glomeruli. (a) Representative immunohistochemical staining for CD8 and PPAR $\alpha$  in vehicle and anti-GBM GN. (b) Numbers of glomerular-infiltrating CD8<sup>+</sup>PPAR $\alpha$ <sup>+</sup> non-T lymphocytes (Lym) and CD8<sup>+</sup>PPAR $\alpha$ <sup>-</sup> Lym were evaluated in anti-GBM GN groups at 7 days (continued)**

expression levels of PPAR $\alpha$  and *Ehhadh* mRNA, induced in anti-GBM GN, were significantly inhibited by the PPAR $\alpha$  agonist (Figure 4m and n, [Supplementary Table S1L](#)).

#### PPAR $\alpha$ directly inhibited the activation of ILC1s and M $\phi$ *in vitro*

We next examined the suppressive effect of PPAR $\alpha$  on ILC1 activation *in vitro*. Sorted CD8<sup>+</sup>ILC1s were stimulated with both IL-12 and IL-18 in the presence or absence of the PPAR $\alpha$  agonist (Figure 5a–d). IFN- $\gamma$  production from ILC1s was significantly enhanced on IL-12 and IL-18 stimulation. This enhancement of ILC1 activation was significantly reduced in the presence of the PPAR $\alpha$  agonist (Figure 5c and d, [Supplementary Table S1N](#)). Similarly, we examined the direct effect of PPAR $\alpha$  on M $\phi$ . The qRT-PCR analyses revealed that the upregulation of *iNOS*, *CXCL9*, *CXCL10*, and *CXCL11* by IFN- $\gamma$  stimulation was significantly suppressed by PPAR $\alpha$  activation, as indicated by upregulation of PPAR $\alpha$  and *Ehhadh* mRNA (Figure 5e, [Supplementary Table S1O](#)). These results suggested that PPAR $\alpha$  directly inhibited the activation of not only ILC1s but also M $\phi$ .

#### PPAR $\alpha$ agonist inhibited the expression of ILC1-related chemokines in GEnCs and podocytes

We next explored the sources of ILC1-related chemokine production. GEnC and podocyte injuries are involved in the progression of anti-GBM GN, and various chemokines are produced from GEnCs and podocytes following glomerular injury.<sup>32–36</sup> In GEnCs, *CXCL9* mRNA, but not *CXCL10* or *CXCL11* mRNA, was significantly upregulated by stimulation of IFN- $\gamma$  (Figure 6a, [Supplementary Table S1P](#)). In contrast, podocytes exhibited significantly increased mRNA expression of *CXCL9*, *CXCL10*, and *CXCL11* following stimulation of IFN- $\gamma$  (Figure 6b, [Supplementary Table S1Q](#)). The upregulation of these chemokines was significantly inhibited in the presence of PPAR $\alpha$  agonist in both GEnCs and podocytes (Figure 6a and b, [Supplementary Table S1P](#) and [Q](#)). However, in GEnCs, the upregulation of *ICAM-1* and *VCAM-1* induced by TNF- $\alpha$  was not suppressed by treatment with the PPAR $\alpha$  agonist ([Supplementary Figure S3B](#), [Supplementary Table S1R](#)), consistent with the findings from analyses of isolated glomeruli from anti-GBM GN rats ([Supplementary Figure S3A](#), [Supplementary Table S1M](#)). These data indicate that PPAR $\alpha$  signaling suppresses the production of ILC1-related chemokines from activated GEnCs, podocytes, and M $\phi$ , thereby resulting in the inhibition of ILC1 migration.

#### ILC1s infiltrated into glomeruli in human anti-GBM GN

To confirm the involvement of ILC1s in the progression of human anti-GBM GN, we analyzed human renal biopsy specimens obtained from patients with anti-GBM GN and compared them with renal tissues from patients who underwent nephrectomy due to renal cell carcinoma (renal control tissues). Human ILC1s were defined as lineage (CD3, CD16, CD19, CD20, CD56, and CD68)-negative and -positive for CD127 and T-bet.<sup>1–3</sup> In human anti-GBM GN samples, approximately 90% of glomeruli showed crescent formation (Figure 7a). Although no ILC1s were detected in the renal control tissues, a considerable number of ILC1s were detected in glomeruli of patients with anti-GBM GN, especially in glomeruli without crescent formation (Figure 7b and c, [Supplementary Table S1S](#)). Indeed, the number of glomerular-infiltrating ILC1s was significantly greater in glomeruli without crescents than in those with crescents (Figure 7d, [Supplementary Table S1T](#)). These data indicate that ILC1s are involved in the progression of anti-GBM GN, especially in the early phase of inflammation. Moreover, PPAR $\alpha$  was expressed in both Lin<sup>–</sup>CD127<sup>+</sup> cells and Lin<sup>–</sup>T-bet<sup>+</sup> cells ([Supplementary Figure S4](#)).

#### DISCUSSION

We report a novel progressive mechanism of anti-GBM GN, in which ILC1s are involved. From the analysis of phenotypic and functional characteristics, we demonstrated the infiltration of ILC1s in the development of anti-GBM GN in rats and humans. Moreover, PPAR $\alpha$  agonist treatment attenuated glomerular injury in anti-GBM GN rats through regulation of ILC1s. These data demonstrate that ILC1s are involved in the progression of anti-GBM GN and could be considered a novel therapeutic target. Furthermore, a strategy targeting PPAR $\alpha$  activation for the regulation of ILC1s might be a useful treatment for anti-GBM GN.

This study is the first, to our knowledge, to identify infiltrating CD8<sup>+</sup>Lym in necrotizing and crescentic glomeruli as ILC1s and report the involvement of ILC1s in the development of anti-GBM GN. Our findings are supported by those of Roan *et al.*,<sup>37</sup> who reported that ILC1s contain CD4<sup>+</sup>CD8<sup>–</sup>, CD4<sup>–</sup>CD8<sup>+</sup>, and CD4<sup>–</sup>CD8<sup>–</sup> populations. Although some populations of NK cells are believed to express CD8, the ILC1s that we identified do not express CD161 (an NK cell marker in rats). Moreover, the expression of Eomes in ILC1s is significantly lower than that in conventional NK cells. Therefore, this population of ILC1s differs

**Figure 3 |** (continued) following the induction of anti-GBM GN. Cell infiltration was quantified by the mean number of these cells per glomerulus in 30 glomerular cross sections (GCs). (c) Quantitative real-time polymerase chain reaction analysis of mRNA for PPAR $\alpha$  and *enoyl-CoA hydratase and 3-hydroxyacyl CoA dehydrogenase* (*Ehhadh*) in isolated glomerular-infiltrating CD8<sup>+</sup>Lym and M $\phi$ . Results are normalized to  $\beta$ -actin and are presented as relative expression levels compared with those of M $\phi$  (set as 1). (d) Quantitative real-time polymerase chain reaction analysis of mRNAs for PPAR $\alpha$  and *Ehhadh* in isolated glomeruli. Results are normalized to  $\beta$ -actin and are presented as relative expression levels compared with those of vehicle group (set as 1). (e–g) Serum creatinine (e) and urinary albumin excretion (f) amounts and frequency of necrotizing and crescentic glomeruli (g) in vehicle or fenofibrate treatment groups on days 3, 5, and 7 following the induction of anti-GBM GN. (g) The frequencies of necrotizing and crescentic glomeruli are expressed as the mean percentage of glomeruli with lesions in 100 glomeruli in each kidney sample. (h) Representative light microscopic findings (periodic acid–Schiff stain). (Continued)

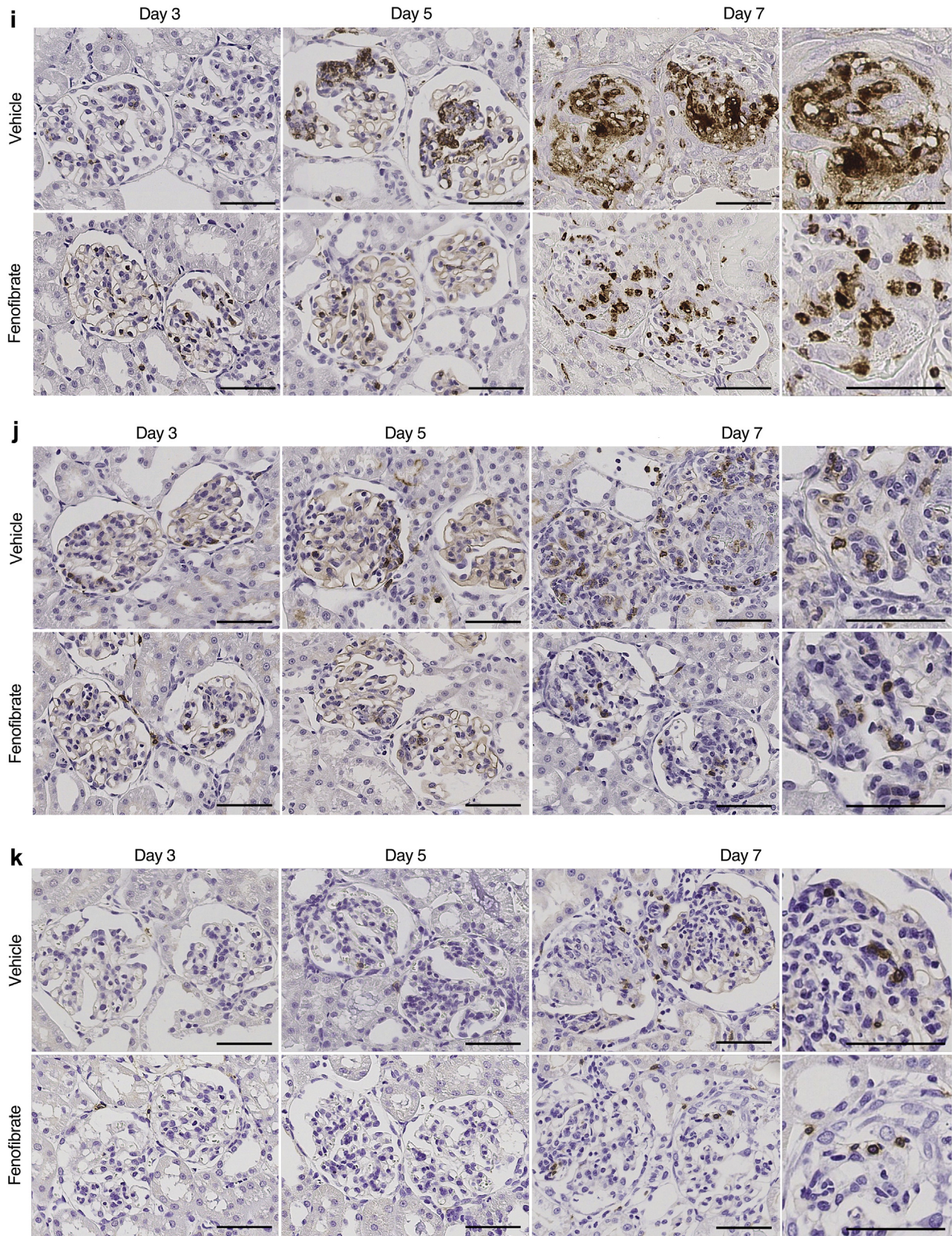


**Figure 3 |** (Continued) (i–k) Representative immunohistochemical staining for CD68 (i), CD8 (j), and CD3 (k) in vehicle or fenofibrate treatment groups on days 3, 5, and 7 following the induction of anti-GBM GN. (Continued)

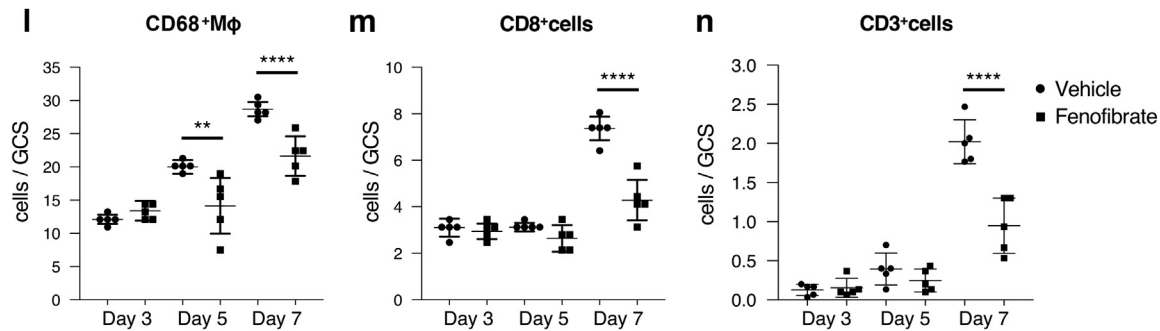


**Figure 3 |** (Continued) (l–m) Numbers of glomerular-infiltrating CD68<sup>+</sup>Mφ (l), CD8<sup>+</sup>Lym (m), and CD3<sup>+</sup> (n) cells were evaluated in vehicle or fenofibrate treatment groups on days 3, 5, and 7 following the induction of anti-GBM GN. Infiltration of CD68<sup>+</sup>Mφ, CD8<sup>+</sup>Lym, and CD3<sup>+</sup> cells was quantified by the mean numbers of CD68-positive, CD8-positive, and CD3-positive cells per glomerulus in 30 GCSs, respectively. Values represent the mean ± SD of evaluations from each group (c: n = 6 per group; b, d–g, l–n: n = 5 per group). \*\**P* < 0.01, \*\*\**P* < 0.005, and \*\*\*\**P* < 0.001. Original magnification ×400 (h–k) and ×600 (a, i–k [day 7 right]). Bar = 50 μm. To optimize viewing of this image, please see the online version of this article at [www.kidney-international.org](http://www.kidney-international.org).

from conventional NK cells. Wu *et al.*<sup>38</sup> reported the identification of a CD8 $\alpha^+$  major histocompatibility complex class II<sup>+</sup> cell with both antigen-presenting functions and NK-like cytotoxicity. In their anti-GBM GN rat model, these cells infiltrated into glomeruli on days 35 to 40 after disease induction and suppressed inflammation by inducing apoptosis in effector CD4<sup>+</sup> T cells. Based on differences in the roles of inflammatory responses and the time phase of infiltration, those cells differ from the ILC1s identified herein. Indeed, in this study, more than 95% of glomerular-infiltrating CD8<sup>+</sup>Lym did not express RT1B (data not shown). Van Kaer *et al.*<sup>39</sup> reported that innate CD8 $\alpha^+$  cells are involved in innate immunity against bacterial infection in both mouse and human intestinal epithelium. Such CD8<sup>+</sup> cells do not express either T cell receptor or CD127 in a major subset of ILC populations and produce IFN- $\gamma$ . However, the same cells express CD103; thus, they differ from the ILC1s described in the current study. In our study, CD127 was not expressed in rat ILC1s (data not shown). However, several investigators have revealed the presence of a subset of ILC1s that do not express CD127 in the liver, salivary gland, or tonsils.<sup>6,40</sup> Further studies are required to clarify the phenotypic differences between rat and human ILCs.

Studies from recent years have shown that ILCs are associated with various inflammatory diseases.<sup>5–8,37</sup> Huang *et al.*<sup>41</sup> and Cao *et al.*<sup>42</sup> recently reported that ILC2s induced by IL-25 or IL-33 treatment attenuated renal ischemic/reperfusion injury by producing large amounts of Th2-related cytokines, such as IL-4 and IL-13, and by inducing alternatively activated Mφ. Furthermore, Riedel *et al.*<sup>43</sup> demonstrated that ILC populations reside in the healthy human kidney and ILC2s are a major ILC subtype in the kidneys of humans and mice. However, the association between ILC1s and kidney diseases has not been clarified. ILC1s play an essential role in the initiation and regulation of inflammation in the innate immune response. In our study, ILC1s infiltrated into glomeruli during early stages of disease in anti-GBM GN rats and appeared within glomeruli in patients with anti-GBM GN. Interestingly, the larger number of ILC1s that infiltrated into

glomeruli without crescents supports a role for ILC1s in the early progression of anti-GBM GN. We also found that ILC1s are the main IFN- $\gamma$ -producing cells in the early phase of anti-GBM GN. IFN- $\gamma$ , a Th1 cytokine, plays an important role in Mφ activation.<sup>44</sup> Following the induction of anti-GBM GN, IFN- $\gamma$  knockout mice developed less severe glomerular injury than wild-type mice by regulating Mφ activation.<sup>45</sup> Phoon *et al.*<sup>46</sup> reported that T-bet knockout anti-GBM GN mice showed attenuated renal injury and a reduction in the number of glomerular-infiltrating Mφ. Because T-bet is an essential transcription factor not only in Th1 cells, but also in ILC1s, the lack of ILC1s may result in the suppression of Mφ activation and attenuation of anti-GBM GN. Previous studies reported that Th1 and Th17 cells were involved in the progression of experimental anti-GBM GN.<sup>16–19</sup> However, in our study, few CD3<sup>+</sup> T cells were detected in the glomeruli in anti-GBM GN, despite the presence of many glomerular-infiltrating CD8<sup>+</sup>ILC1s. This may have occurred because our experimental model shows only the early phase of the immune response (i.e., the innate immune response) in anti-GBM GN. Moreover, CD8<sup>+</sup>Lym play an important role in the development of anti-GBM GN in rats.<sup>11,12</sup> Therefore, these results lead us to believe that ILC1s could serve as a novel therapeutic target in the early phase of anti-GBM GN.

PPAR $\alpha$  agonists reduce proinflammatory cytokines, including TNF- $\alpha$  and IFN- $\gamma$ , by regulating the transcription of their genes by repressing nuclear factor- $\kappa$ B and activator protein-1 signaling in inflammatory-induced disorders.<sup>30,47–49</sup> In this study, the PPAR $\alpha$  agonist directly inhibited the activation of ILC1s induced by IL-12 and IL-18 (Figure 5a–d). Zhang *et al.*<sup>29</sup> demonstrated that PPAR $\alpha$  signaling suppresses IFN- $\gamma$  production from CD4<sup>+</sup>, CD8<sup>+</sup> T, and NK T cells. However, such suppressive effects were not observed in NK cells. Thus, the CD8<sup>+</sup>ILC1s described in the current study differ from NK cells, and we reveal a novel anti-inflammatory mechanism of PPAR $\alpha$  via the regulation of ILC1s. Previous studies have shown the anti-inflammatory effects of PPAR $\alpha$  on Mφ.<sup>50,51</sup> In this study, we have similarly shown that the administration of a PPAR $\alpha$  agonist directly inhibited

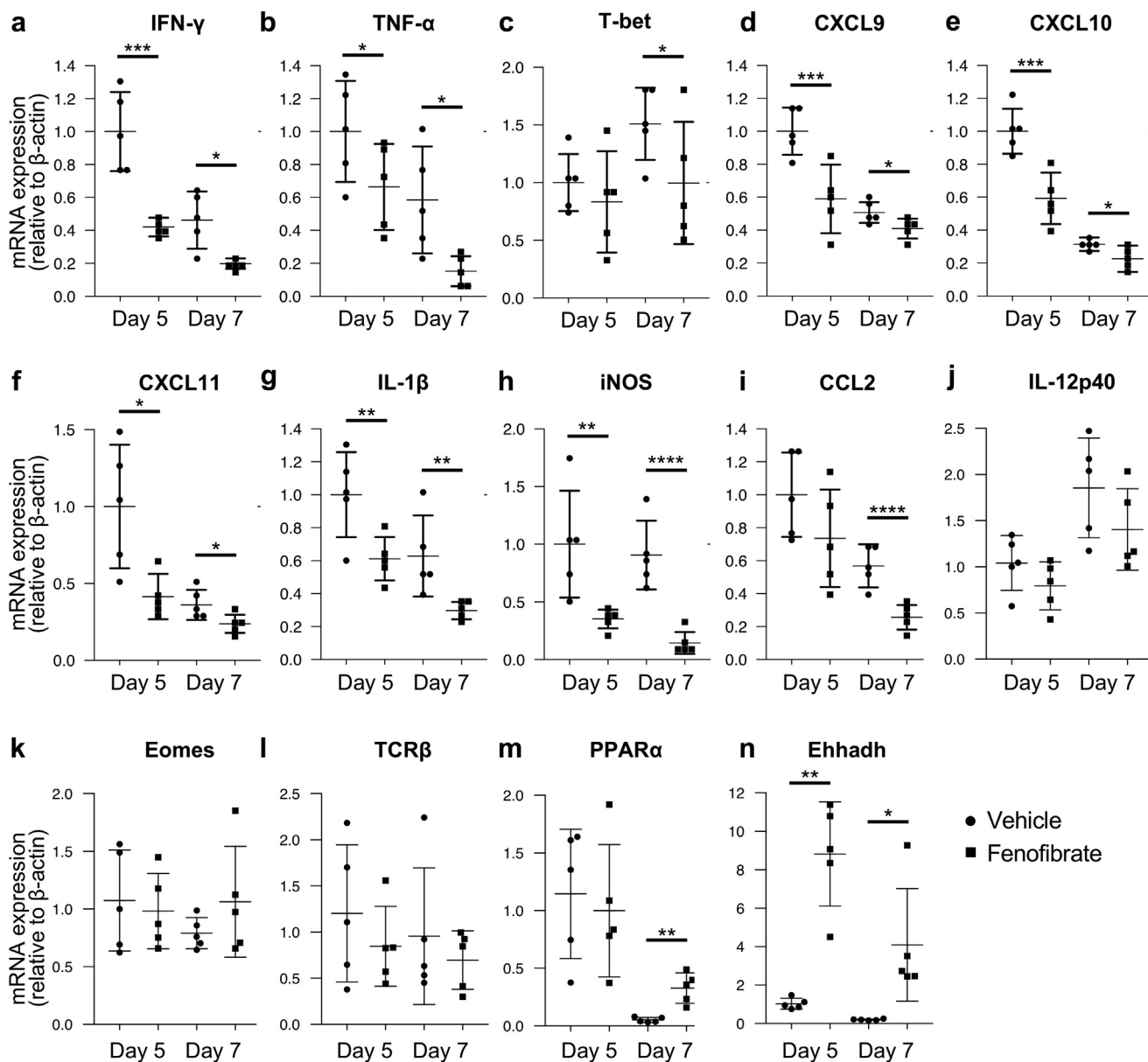


**Figure 4 | Treatment with a peroxisome proliferator-activated receptor- $\alpha$  (PPAR $\alpha$ ) agonist suppressed the glomerular expression of group 1 innate lymphoid cell-related cytokines and chemokines *in vivo*.** Quantitative real-time polymerase chain reaction analysis of mRNA for interferon- $\gamma$  (IFN- $\gamma$ ) (a), tumor necrosis factor- $\alpha$  (TNF- $\alpha$ ) (b), T-box factor expressed in T cells (T-bet) (c), CXC chemokine ligand 9 (CXCL9) (d), CXCL10 (e), CXCL11 (f), interleukin-1  $\beta$  (IL-1 $\beta$ ) (g), inducible nitric oxide synthase (iNOS) (h), C-C motif chemokine ligand 2 (CCL2) (i), IL-12p40 (j), eomesodermin (Eomes) (k), T-cell receptor  $\beta$  (TCR $\beta$ ) (l), PPAR $\alpha$  (m), and enoyl-CoA hydratase and 3-hydroxyacyl CoA dehydrogenase (Ehhadh) (n) in isolated glomeruli of vehicle- or fenofibrate-treated rats on days 5 and 7 following the induction of anti-glomerular basement membrane glomerulonephritis. Results are normalized to  $\beta$ -actin and are presented as the relative expression compared with that of the vehicle group on day 5 (set as 1). Values represent the mean  $\pm$  SD of evaluations from each group ( $n = 5$  per group). \* $P < 0.05$ , \*\* $P < 0.01$ , \*\*\* $P < 0.005$ , and \*\*\*\* $P < 0.001$ .

M $\phi$  activation by IFN- $\gamma$  stimulation. These findings suggested that PPAR $\alpha$  serves to inhibit the activation of innate immune cells, such as M $\phi$  and ILCs, in inflammatory diseases.

Although treatment with fenofibrate significantly downregulated glomerular expression of inflammatory cytokine and chemokine mRNAs in this study, there was a delay between downregulation of these mRNAs and downregulation of T-bet mRNA. We demonstrated that CD8<sup>+</sup>ILC1s composed the majority of IFN- $\gamma$ -expressing cells in the early

phase of anti-GBM GN. Fenofibrate directly inhibited cytokine and chemokine production from CD8<sup>+</sup>ILC1s, M $\phi$ , podocytes, and GEnCs. Thereafter, recruitment of CD8<sup>+</sup>ILC1s was indirectly inhibited through the fenofibrate-induced suppression of ILC1-related chemokines. Although there were no significant statistical differences between the vehicle and fenofibrate groups in the number of glomerular-infiltrating CD8<sup>+</sup>Lym or in the expression of T-bet mRNA on day 5, the mean values of these variables showed a slight

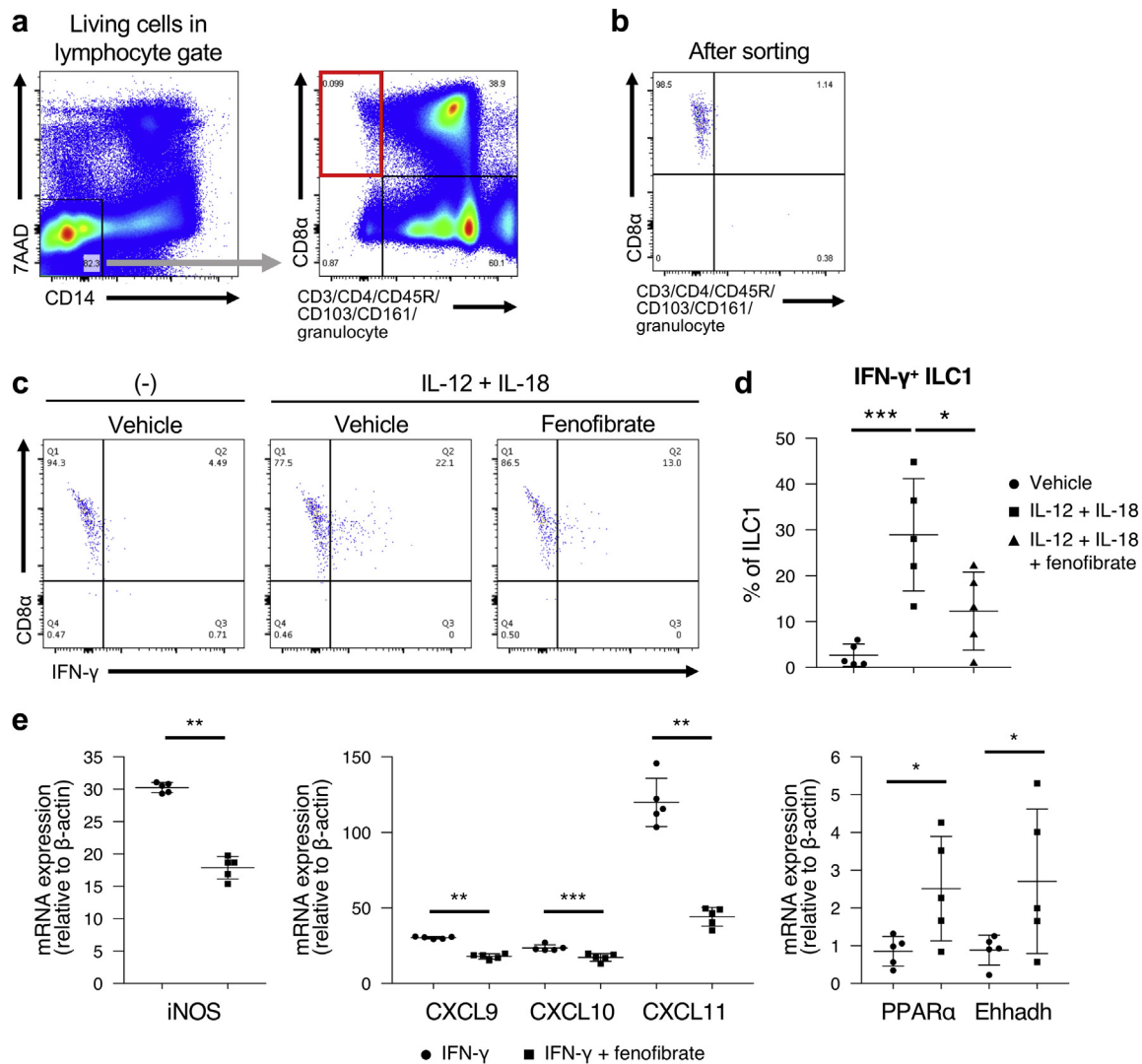


**Figure 5 | Peroxisome proliferator-activated receptor- $\alpha$  (PPAR $\alpha$ ) directly inhibited the activation of group 1 innate lymphoid cells (ILC1s) and macrophages *in vitro*.** (a) Representative flow cytometric analyses showing the gating strategy to sort living CD8 $\alpha$ <sup>+</sup> lineage marker-negative (CD3<sup>−</sup>CD4<sup>−</sup>CD14<sup>−</sup>CD45R<sup>−</sup>CD103<sup>−</sup>CD161<sup>−</sup>granulocyte<sup>−</sup>) ILC1s (red outlined area, right panel) from rat splenocytes. (b) Representative flow cytometric analyses of sorted CD8 $\alpha$ <sup>+</sup> ILC1s. CD8 $\alpha$ <sup>+</sup> ILC1 purity was more than 95%. (c) Interferon- $\gamma$  (IFN- $\gamma$ ) production of highly purified spleen CD8 $\alpha$ <sup>+</sup> ILC1s after stimulation for 16 hours with or without the combination of interleukin-12 (IL-12) and IL-18, as assessed by flow cytometry. Numbers in gates (outlined areas) and quadrants indicate the percentages of cells in each. (d) Frequencies of IFN- $\gamma$ -positive ILC1s in the vehicle group and IL-12 and IL-18 stimulation groups with or without fenofibrate treatment. (e) Quantitative real-time polymerase chain reaction analysis of mRNAs for inducible nitric oxide synthase (*iNOS*), ILC1-related chemokines, *PPAR $\alpha$* , and *enoyl-CoA hydratase and 3-hydroxyacyl CoA dehydrogenase* (*Ehhadh*) in cultured macrophages. Results are normalized to  $\beta$ -actin and are presented as relative expression levels compared with those of unstimulated macrophages (set as 1). Values represent the mean  $\pm$  SD of evaluations from each group ( $n = 5$  per group). \* $P < 0.05$ , \*\* $P < 0.01$ , and \*\*\* $P < 0.005$ . CXCL9, CXC chemokine ligand 9.

tendency toward reduction in the fenofibrate group. These results suggest that fenofibrate predominantly affects the expression of ILC1-related cytokines and chemokines rather than the recruitment of T-bet<sup>+</sup> cells (e.g., CD8<sup>+</sup> ILC1s).

Several studies have reported a protective role for PPAR $\alpha$  in podocytes through preservation of nephrin expression in glomerular injury models.<sup>52,53</sup> However, few reports are available regarding the anti-inflammatory roles of PPAR $\alpha$  in GEnCs and podocytes. The production of chemokines from endothelial cells and podocytes leads to local recruitment of inflammatory cells, while ILC1s reportedly express CXC

chemokine receptor 3, in a manner similar to that of T cells.<sup>4,34,37,54–56</sup> In this study, PPAR $\alpha$  treatment inhibited ILC and T-cell migration into glomeruli via downregulation of ILC1-related chemokines in glomeruli, including GEnCs and podocytes. Further studies are needed to reveal the therapeutic effect of PPAR $\alpha$  on lymphocytes, including ILC1s, in various inflammation-induced disorders.

Our study had several important limitations. First, although we evaluated the effects of PPAR $\alpha$  on ILC1 and M $\phi$ , no other leukocytes were evaluated. ILC1-related chemokines are indeed produced by M $\phi$ , podocytes, and GEnCs; however,

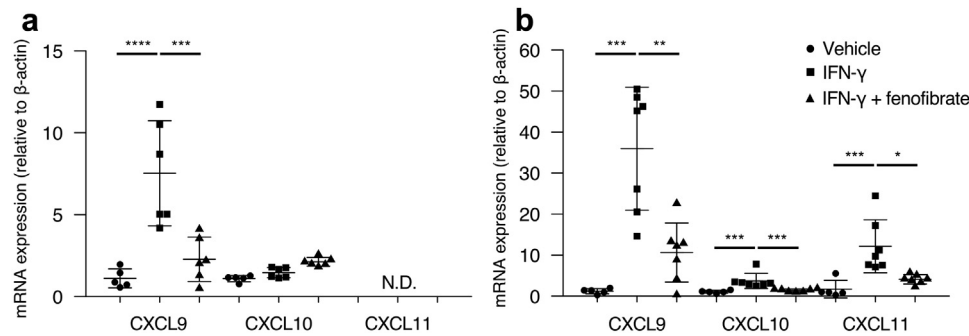


**Figure 6 | Treatment with peroxisome proliferator-activated receptor- $\alpha$  agonist inhibited the expression of group 1 innate lymphoid cell-related chemokines in glomerular endothelial cells and podocytes.** Quantitative real-time polymerase chain reaction analysis of mRNAs for group 1 innate lymphoid cell-related chemokines, including *CXC chemokine ligand 9* (CXCL9), CXCL10, and CXCL11, in rat glomerular endothelial cells (a) and mouse podocytes (b). Results are normalized to  $\beta$ -actin and are presented as relative expression compared with that of the vehicle group (set as 1). Values represent the mean  $\pm$  SD of evaluations from each group (glomerular endothelial cells,  $n = 5$  per vehicle group;  $n = 6$  per group for other groups. Podocytes,  $n = 5$  per vehicle group;  $n = 7$  per group for other groups). \* $P < 0.05$ , \*\* $P < 0.01$ , \*\*\* $P < 0.005$ , and \*\*\*\* $P < 0.001$ . IFN- $\gamma$ , interferon- $\gamma$ ; N.D., not detected.

they are also produced by dendritic cells and neutrophils.<sup>57,58</sup> Several studies have reported that PPAR $\alpha$  regulates the activation of T cells and dendritic cells.<sup>59–61</sup> Moreover, the activation of neutrophils is reportedly regulated by NF- $\kappa$ B signaling, which can be inhibited by PPAR $\alpha$ .<sup>30,47–49,62</sup> Although ILC1s, M $\phi$ , podocytes, and GEnCs were the focus of this study because of their relevance to the early progression of anti-GBM GN,<sup>9–14,32,33</sup> other leukocytes may be regulated by PPAR $\alpha$ . Second, we could not evaluate IL-18 expression in anti-GBM GN. IL-18 is a member of the highly proinflammatory IL-1 family of cytokines; it is synthesized as a biologically inactive precursor protein, which is cleaved prior to secretion as a bioactive cytokine.<sup>63</sup> Therefore, the level of IL-18 mRNA does not accurately reflect inflammatory status. Previous studies demonstrated that IL-12 and IL-18 were needed to activate ILC1s;<sup>1–5</sup> thus, IL-18 was administered to cultured ILC1s with IL-12 in this study. Finally, we examined only the preventive administration of a PPAR $\alpha$  agonist. Further studies are therefore needed to elucidate the therapeutic effect of PPAR $\alpha$  in advanced anti-GBM GN.

In conclusion, we determined the functional significance of ILC1s in the progression of anti-GBM GN and the therapeutic effects of PPAR $\alpha$  on ILC1s. ILC1s are novel immune cells in the field of renal disease and thus the clarification of ILC1s and the progression of renal disease, including GN, may lead to the development of a novel specific therapy for these diseases.

## METHODS

Full methods are available in the [Supplementary Methods](#).

### Rat models

We used a Wistar Kyoto rat model of anti-GBM GN, as previously published.<sup>9,10</sup> To investigate the CD8<sup>+</sup>Lym profile, 5 rats were killed on day 7 following injection of the anti-GBM antibody. To evaluate the effects of PPAR $\alpha$ , rats were treated with oral fenofibrate (300 mg/kg per body weight per day) (Wako, Osaka, Japan) or vehicle once

daily beginning 1 day before injection of the anti-GBM antibody for killing.

### Histopathology and immunohistochemistry

Kidney tissues were fixed in 10% neutral-buffered formalin and embedded in paraffin for light microscopy examination. Tissue sections were stained with hematoxylin and eosin and periodic acid-Schiff for histopathological examination. For immunohistochemistry, paraffin-embedded tissue sections were stained using Histofine Simple Stain Rat MAX PO (MULTI; Nichirei, Tokyo, Japan) following the protocol of the standard avidin-biotin-peroxidase complex technique. For immunofluorescence staining in rats, 4- $\mu$ m frozen sections were stained by the standard indirect and direct technique. In human kidney biopsy specimens, immunofluorescence multiplex staining was performed with the PerkinElmer Opal Kit (Perkin-Elmer, Waltham, MA) as previously described.<sup>64</sup> Antibody details can be found in the [Supplementary Methods](#).

### Quantification of serum creatinine and albuminuria

Serum creatinine was measured using The DetectX Serum Creatinine kits from Arbor Assays (Ann Arbor, MI). Albuminuria was determined by a Rat Albumin ELISA Kit from Bethyl Laboratories (Montgomery, TX).

### Isolation of rat glomeruli

Glomeruli were isolated by a differential sieving method from harvested kidneys as described previously.<sup>65</sup> Under light microscopy, tubular contamination was <5%.

### Cell preparation

Disrupted spleens and isolated glomeruli were digested for 30 minutes at 37 °C in RPMI 1640 medium (Wako) supplemented with collagenase D (1 mg/ml; Roche Life Science, Mannheim, Germany) and DNase I (100  $\mu$ g/ml; Sigma-Aldrich, St. Louis, MO). Next, the digested cell suspension was passed through a 40- $\mu$ m cell strainer. The panning method was performed to enrich CD8<sup>+</sup>Lym from splenocytes according to Wysocki and Sato.<sup>66</sup>

### Flow cytometry and cell sorting

For cell surface labeling, cell suspensions were stained with fluorochrome-bound antibodies for 30 minutes at 4 °C. For

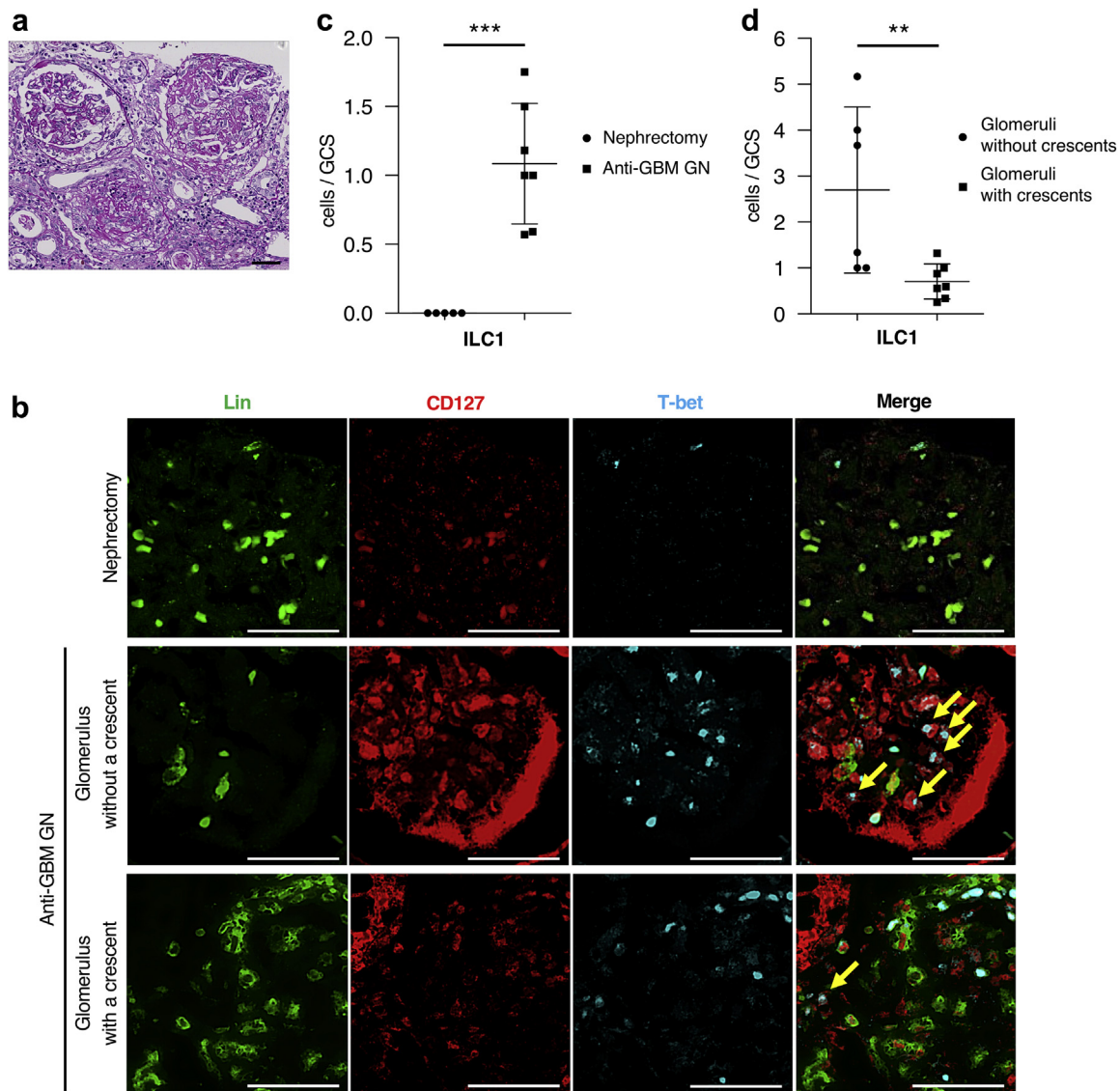


**Figure 7 | Group 1 innate lymphoid cells (ILC1s) infiltrated into glomeruli in human anti-glomerular basement membrane (anti-GBM) glomerulonephritis (GN).** (a) Representative light microscopic findings in kidney biopsy specimens of patients with anti-GBM GN (periodic acid–Schiff stain). (b) Representative immunofluorescence staining for lineage marker (Lin) (CD3, CD16, CD19, CD20, CD56, and CD68; green), CD127 (red), and T-box factor expressed in T cells (T-bet) (cyan) in unaffected renal tissue from patients undergoing total nephrectomy due to renal cell carcinoma (top), glomeruli without a crescent (middle), and with (bottom) a crescent in human anti-GBM GN. Arrows indicate ILC1s (Lin<sup>+</sup>CD127<sup>+</sup>T-bet<sup>+</sup> cells). Original magnification  $\times 100$  (a) and  $\times 400$  (b). Bar = 50  $\mu$ m. (c) Number of glomerular-infiltrating ILC1s in unaffected renal tissue and human anti-GBM GN. (d) Number of glomerular-infiltrating ILC1s in glomeruli with or without crescents in human anti-GBM GN. Values represent the mean  $\pm$  SD of evaluations from each group ( $n = 5$  per nephrectomy group,  $n = 7$  per anti-GBM group,  $n = 6$  per glomeruli-without-crescents group, and  $n = 7$  per glomeruli-with-crescents group).  $**P < 0.01$  and  $***P < 0.005$ . GCS, glomerular cross section. To optimize viewing of this image, please see the online version of this article at [www.kidney-international.org](http://www.kidney-international.org).

intracellular cytokine analysis, monensin (35 mg/kg per body weight), obtained from Sigma-Aldrich, was administered i.p. 6 hours before killing. Intracellular staining was performed using an Intracellular Fixation & Permeabilization Buffer Set (Thermo Fisher Scientific, Waltham, MA) according to the manufacturer's instructions. Data were collected by FACSCanto II (BD Biosciences, San Jose, CA), and cells were sorted by FACSARIA II (BD Biosciences). Data were analyzed by FlowJo software 10.4.2 (BD Biosciences). Antibody details can be found in the [Supplementary Methods](#).

#### qRT-PCR analyses

Total RNA was extracted by ISOGEN II (Nippon Gene, Tokyo, Japan) and transcribed into cDNA by the High Capacity cDNA Reverse Transcription Kit (Applied Biosystems, Foster City, CA). A cDNA copy of sorted cells was created with the CellAmp Whole Transcriptome Amplification Kit (Takara Bio, Siga, Japan) according to the manufacturer's instructions. qRT-PCR was performed with THUNDERBIRD SYBR qPCR Mix (TOYOBO, Osaka, Japan) using a QuantStudio 5 (Applied Biosystems). The primer sequences used for qRT-PCR are shown in [Supplementary Table S2](#).

## Cell culture experiments

Cyclin-dependent kinase 4-transformed mouse podocytes were provided by Dr. Jeffrey B. Kopp (University College London, UK) and generated according to the protocol of Sakairi *et al.*<sup>67</sup> Podocytes were incubated with recombinant mouse IFN- $\gamma$  (10 ng/ml) from Peprotech (Rocky Hill, NJ). Rat primary kidney GEnCs were purchased from Cell Biologics (Chicago, IL). GEnCs were incubated with recombinant rat IFN- $\gamma$  (10 ng/ml) or TNF- $\alpha$  (20 ng/ml) from BioLegend (San Diego, CA). Purified CD8<sup>+</sup>Lym were stimulated with combinations of recombinant rat IL-12 (50 ng/ml) and IL-18 (50 ng/ml) from Genscript (Piscataway, NJ). Rat M $\phi$  were induced from bone marrow cells collected from femur and tibia of normal Wistar Kyoto rats in accordance with the protocol of Avni *et al.*<sup>68</sup> M $\phi$  were incubated with recombinant rat IFN- $\gamma$  (10 ng/ml). Cells were incubated for 24 hours in the absence or presence of 10  $\mu$ mol/l fenofibrate.

## Human material

Human kidney biopsy specimens were obtained from 7 patients who underwent a kidney biopsy and were diagnosed with anti-GBM GN by a pathologist in our hospital. The unaffected tissues of kidneys from 5 patients who underwent total nephrectomy due to renal cell carcinoma were used as control renal tissues. The study was performed in accordance with the Declaration of Helsinki and was approved by the ethical committee of our hospital (30-07965).

## Statistical analyses

Continuous variables are expressed as the mean  $\pm$  SD. The normality of the quantitative data was checked by the Kolmogorov-Smirnov test. For normally distributed variables, Student's *t*-test was used to compare variables between 2 groups; 1-way analysis of variance with Dunnett's *post hoc* test was used to compare variables among 3 or more groups. For nonparametric variables, the Mann-Whitney *U* test was used to compare variables between 2 groups; the Kruskal-Wallis test with Dunn's *post hoc* test was used to compare variables among 3 or more groups. All statistical analyses were performed using the SPSS version 25.0 statistical software package (IBM Corp., Armonk, NY).

## DISCLOSURE

All the authors declared no competing interests.

## ACKNOWLEDGMENTS

We express our special thanks to Mr. Takashi Arai, Ms. Mitue Kataoka, Kyoko Wakamatsu, Arimi Ishikawa, Naomi Kuwahara, and Masumi Shimizu for their expert technical assistance. This work was supported by LEGEND Research Grant 2016 and the Jikei University Research Fund for Graduate Students. Parts of this study were presented at the 51th Annual Meeting of American Society of Nephrology Kidney Week 2017, November 2, 2017, New Orleans, LA; the 55th European Renal Association–European Dialysis Transplant Association Congress, May 25, 2018, Denmark, Copenhagen; and the 61th Annual Meeting of Japanese Society of Nephrology, June 9, 2018, Niigata, Japan.

## SUPPLEMENTARY MATERIAL

### Supplementary Methods.

**Figure S1.** (A) Representative flow cytometric analyses of glomeruli isolated from Wistar Kyoto rats on day 7 following the induction of anti-glomerular basement membrane glomerulonephritis. Right panel shows the expression of CD8 $\alpha$  on CD45<sup>+</sup> lineage marker (Lin)<sup>−</sup> (CD3<sup>−</sup>CD4<sup>−</sup>CD14<sup>−</sup>CD45R<sup>−</sup>CD103<sup>−</sup>CD161<sup>−</sup>granulocyte<sup>−</sup>)

glomerular-infiltrating leukocytes (red outlined area, left panel). Macrophages (M $\phi$ ) were defined as CD14<sup>+</sup> leukocytes (black outline area, left panel). (B) Frequency of CD8<sup>+</sup>Lin<sup>−</sup> cells and CD8<sup>−</sup>Lin<sup>−</sup> cells in glomerular-infiltrating Lin<sup>−</sup> cells. Lym, non-T lymphocytes.

**Figure S2.** The phenotype of CD8<sup>+</sup> non-T lymphocytes (CD8<sup>+</sup>Lym) differs distinctly from that of natural killer (NK) cells. (A) Representative flow cytometric analyses showing the gating strategy to sort out living CD161<sup>+</sup> lineage marker (Lin)<sup>−</sup> (CD3<sup>−</sup>CD4<sup>−</sup>CD14<sup>−</sup>CD45R<sup>−</sup>CD103<sup>−</sup>granulocyte<sup>−</sup>) NK cells (black lined area, right panel) from rat splenocytes. (B) Quantitative real-time polymerase chain reaction analysis of mRNAs for *eomesodermin* (*Eomes*) and *T-box factor expressed in T cells* (*T-bet*) in sorted glomerular-infiltrating CD8<sup>+</sup>Lym and spleen NK cells. Results are normalized to  $\beta$ -actin and are presented as relative expression compared with that of CD8<sup>+</sup>Lym (set as 1). Values represent the mean  $\pm$  SD of evaluations from CD8<sup>+</sup>Lym and NK cells (*n* = 6 per group). \**P* < 0.05.

**Figure S3.** Peroxisome proliferator-activated receptor- $\alpha$  was unable to suppress the activation of glomerular endothelial cells (GEnCs) both *in vitro* and *in vivo*. Quantitative real-time polymerase chain reaction analysis of mRNAs for *intercellular adhesion molecule-1* (*ICAM-1*) and *vascular cell adhesion molecule-1* (*VCAM-1*) in (A) isolated glomeruli and (B) cultured rat GEnCs. Results are normalized to  $\beta$ -actin and are presented as relative expression compared with that of the vehicle group on day 5 and unstimulated GEnCs (set as 1), respectively. Values represent the mean  $\pm$  SD of evaluations from each group (isolated glomeruli, *n* = 5 per group; GEnCs, *n* = 5 per group). TNF- $\alpha$ , tumor necrosis factor- $\alpha$ .

**Figure S4.** Representative immunofluorescence staining for lineage marker (Lin) (CD3, CD16, CD19, CD20, CD56, and CD68; green), peroxisome proliferator-activated receptor- $\alpha$  (PPAR $\alpha$ ) (cyan), and CD127 (A) or T-box factor expressed in T cells (T-bet) (B) (red) in human anti-glomerular basement membrane glomerulonephritis. Original magnification  $\times$ 400. Arrows indicate Lin<sup>−</sup>CD127<sup>+</sup>PPAR $\alpha$ <sup>+</sup> cells (A) and Lin<sup>−</sup>T-bet<sup>+</sup>PPAR $\alpha$ <sup>+</sup> cells (B). Bar = 50  $\mu$ m.

**Table S1.** The numerical values corresponding to each figure.

**Table S2.** Quantitative real-time polymerase chain reaction primer sequences.

Supplementary material is linked to the online version of the paper at [www.kidney-international.org](http://www.kidney-international.org).

## REFERENCES

- Spits H, Di Santo JP. The expanding family of innate lymphoid cells: regulators and effectors of immunity and tissue remodeling. *Nat Immunol.* 2011;12:21–27.
- Eberl G, Colonna M, Di Santo JP, McKenzie AN. Innate lymphoid cells. Innate lymphoid cells: a new paradigm in immunology. *Science.* 2015;348:aaa6566.
- Spits H, Artis D, Colonna M, et al. Innate lymphoid cells—a proposal for uniform nomenclature. *Nat Rev Immunol.* 2013;13:145–149.
- Cortez VS, Robinette ML, Colonna M. Innate lymphoid cells: new insights into function and development. *Curr Opin Immunol.* 2015;32:71–77.
- Bernink JH, Peters CP, Munneke M, et al. Human type 1 innate lymphoid cells accumulate in inflamed mucosal tissues. *Nat Immunol.* 2013;14:221–229.
- Fuchs A, Vermi W, Lee JS, et al. Intraepithelial type 1 innate lymphoid cells are a unique subset of IL-12- and IL-15-responsive IFN- $\gamma$ -producing cells. *Immunity.* 2013;38:769–781.
- Villanova F, Flutter B, Tosi I, et al. Characterization of innate lymphoid cells in human skin and blood demonstrates increase of Nkp44+ ILC3 in psoriasis. *J Invest Dermatol.* 2013;134:984–991.
- Yang Z, Tang T, Wei X, et al. Type 1 innate lymphoid cells contribute to the pathogenesis of chronic hepatitis B. *Innate Immun.* 2015;21:665–673.
- Fujita E, Shimizu A, Masuda Y, et al. Statin attenuates experimental anti-glomerular basement membrane glomerulonephritis together with the augmentation of alternatively activated macrophages. *Am J Pathol.* 2010;177:1143–1154.

10. Aki K, Shimizu A, Masuda Y, et al. ANG II receptor blockade enhances anti-inflammatory macrophages in anti-glomerular basement membrane glomerulonephritis. *Am J Physiol Renal Physiol*. 2010;298:F870–F882.
11. Kawasaki K, Yaoita E, Yamamoto T, et al. Depletion of CD8 positive cells in nephrotoxic serum nephritis of WKY rats. *Kidney Int*. 1992;41:1517–1526.
12. Fujinaka H, Yamamoto T, Feng L, et al. Crucial role of CD8-positive lymphocytes in glomerular expression of ICAM-1 and cytokines in crescentic glomerulonephritis of WKY rats. *J Immunol*. 1997;158:4978–4983.
13. Fujinaka H, Yamamoto T, Takeya M, et al. Suppression of anti-glomerular basement membrane nephritis by administration of anti-monocyte chemoattractant protein-1 antibody in WKY rats. *J Am Soc Nephrol*. 1997;8:1174–1178.
14. Isome M, Fujinaka H, Adhikary LP, et al. Important role for macrophages in induction of crescentic anti-GBM glomerulonephritis in WKY rats. *Nephrol Dial Transplant*. 2004;19:2997–3004.
15. Nikolic-Paterson DJ, Atkins RC. The role of macrophages in glomerulonephritis. *Nephrol Dial Transplant*. 2001;16(suppl 5):3–7.
16. Tipping PG, Holdsworth SR. T cells in crescentic glomerulonephritis. *J Am Soc Nephrol*. 2006;17:1253–1263.
17. Artinger K, Kirsch AH, Artinger I, et al. Innate and adaptive immunity in experimental glomerulonephritis: a pathfinder tale. *Pediatr Nephrol*. 2017;32:943–947.
18. Hopfer H, Holzer J, Hunemörder S, et al. Characterization of the renal CD4+ T-cell response in experimental autoimmune glomerulonephritis. *Kidney Int*. 2012;82:60–71.
19. Zhang R, Li Q, Chuang PY, et al. Regulation of pathogenic Th17 cell differentiation by IL-10 in the development of glomerulonephritis. *Am J Pathol*. 2013;183:402–412.
20. Derosa G, Sahebkar A, Maffioli P. The role of various peroxisome proliferator-activated receptors and their ligands in clinical practice. *J Cell Physiol*. 2018;233:153–161.
21. Arima T, Uchiyama M, Nakano Y, et al. Peroxisome proliferator-activated receptor alpha agonist suppresses neovascularization by reducing both vascular endothelial growth factor and angiopoietin-2 in corneal alkali burn. *Sci Rep*. 2017;7:17763.
22. Marx N, Duez H, Fruchart J-CC, et al. Peroxisome proliferator-activated receptors and atherogenesis: regulators of gene expression in vascular cells. *Circ Res*. 2004;94:1168–1178.
23. Sato K, Sugawara A, Kudo M, et al. Expression of peroxisome proliferator-activated receptor isoform proteins in the rat kidney. *Hypertens Res*. 2004;27:417–425.
24. Antonelli A, Ferrari SM, Frascerra S, et al. CXCL9 and CXCL11 chemokines modulation by peroxisome proliferator-activated receptor-alpha agonists secretion in Graves' and normal thyrocytes. *J Clin Endocrinol Metab*. 2010;95:E413–E420.
25. Antonelli A, Ferrari SM, Frascerra S, et al. Peroxisome proliferator-activated receptor alpha agonists modulate Th1 and Th2 chemokine secretion in normal thyrocytes and Graves' disease. *Exp Cell Res*. 2011;317:1527–1533.
26. Lee JW, Bajwa PJ, Carson MJ, et al. Fenofibrate represses interleukin-17 and interferon-gamma expression and improves colitis in interleukin-10-deficient mice. *Gastroenterology*. 2007;133:108–123.
27. Manoharan I, Suryawanshi A, Hong Y, et al. Homeostatic PPARalpha signaling limits inflammatory responses to commensal microbiota in the intestine. *J Immunol*. 2016;196:4739–4749.
28. Saga D, Sakatsume M, Ogawa A, et al. Bezafibrate suppresses rat anti-glomerular basement membrane crescentic glomerulonephritis. *Kidney Int*. 2005;67:1821–1829.
29. Zhang MA, Ahn JJ, Zhao FL, et al. Antagonizing peroxisome proliferator-activated receptor alpha activity selectively enhances Th1 immunity in male mice. *J Immunol*. 2015;195:5189–5202.
30. Staels B, Koenig W, Habib A, et al. Activation of human aortic smooth-muscle cells is inhibited by PPAR $\alpha$  but not by PPAR $\gamma$  activators. *Nature*. 1998;393:790–793.
31. Kamijo Y, Hora K, Nakajima T, et al. Peroxisome proliferator-activated receptor alpha protects against glomerulonephritis induced by long-term exposure to the plasticizer di-(2-ethylhexyl)phthalate. *J Am Soc Nephrol*. 2007;18:176–188.
32. Shimizu A, Masuda Y, Mori T, et al. Vascular endothelial growth factor165 resolves glomerular inflammation and accelerates glomerular capillary repair in rat anti-glomerular basement membrane glomerulonephritis. *J Am Soc Nephrol*. 2004;15:2655–2665.
33. Thorner PS, Ho M, Eremina V, et al. Podocytes contribute to the formation of glomerular crescents. *J Am Soc Nephrol*. 2008;19:495–502.
34. Banas MC, Banas B, Hudkins KL, et al. TLR4 links podocytes with the innate immune system to mediate glomerular injury. *J Am Soc Nephrol*. 2008;19:704–713.
35. Panzer U, Steinmetz OM, Reinking RR, et al. Compartment-specific expression and function of the chemokine IP-10/CXCL10 in a model of renal endothelial microvascular injury. *J Am Soc Nephrol*. 2006;17:454–464.
36. Segerer S, Nelson PJ, Schlondorff D. Chemokines, chemokine receptors, and renal disease: from basic science to pathophysiologic and therapeutic studies. *J Am Soc Nephrol*. 2000;11:152–176.
37. Roan F, Stoklasek TA, Whalen E, et al. CD4+ group 1 innate lymphoid cells (ILC) form a functionally distinct ILC subset that is increased in systemic sclerosis. *J Immunol*. 2016;196:2051–2062.
38. Wu J, Carlock C, Ross A, et al. CD8 $\alpha\alpha$ +MHC class II+ cell with the capacity to terminate autoimmune inflammation is a novel antigen-presenting NK-like cell in rats. *J Immunol*. 2016;197:4274–4282.
39. Van Kaer L, Algood HMS, Singh K, et al. CD8 $\alpha\alpha$ + innate-type lymphocytes in the intestinal epithelium mediate mucosal immunity. *Immunity*. 2014;41:451–464.
40. Jiao Y, Huntington ND, Belz GT, et al. Type 1 innate lymphoid cell biology: lessons learnt from natural killer cells. *Front Immunol*. 2016;7:426.
41. Huang Q, Niu Z, Tan J, et al. IL-25 elicits innate lymphoid cells and multipotent progenitor type 2 cells that reduce renal ischemic/reperfusion injury. *J Am Soc Nephrol*. 2015;26:2199–2211.
42. Cao Q, Wang Y, Niu Z, et al. Potentiating tissue-resident type 2 innate lymphoid cells by IL-33 to prevent renal ischemia-reperfusion injury. *J Am Soc Nephrol*. 2018;29:961–976.
43. Riedel JH, Becker M, Kopp K, et al. IL-33-mediated expansion of type 2 innate lymphoid cells protects from progressive glomerulosclerosis. *J Am Soc Nephrol*. 2017;28:2068–2080.
44. Huang S, Hendriks W, Althage A, et al. Immune response in mice that lack the interferon-gamma receptor. *Science*. 1993;259:1742–1745.
45. Kitching AR, Holdsworth SR, Tipping PG. IFN-gamma mediates crescent formation and cell-mediated immune injury in murine glomerulonephritis. *J Am Soc Nephrol*. 1999;10:752–759.
46. Phoon RK, Kitching AR, Odobasic D, et al. T-bet deficiency attenuates renal injury in experimental crescentic glomerulonephritis. *J Am Soc Nephrol*. 2008;19:477–485.
47. Duan SZ, Usher MG, Mortensen RM. PPARs: the vasculature, inflammation and hypertension. *Curr Opin Nephrol Hypertens*. 2009;18:128–133.
48. Silva A, Peixoto C. Role of peroxisome proliferator-activated receptors in non-alcoholic fatty liver disease inflammation. *Cell Mol Life Sci*. 2018;75:1–11.
49. Hashimoto K, Kamijo Y, Nakajima T, et al. PPARalpha activation protects against anti-Thy1 nephritis by suppressing glomerular NF-kappaB signaling. *PPAR Res*. 2012;2012:976089.
50. Crisafulli C, Cuzzocrea S. The role of endogenous and exogenous ligands for the peroxisome proliferator-activated receptor alpha (Ppar- $\alpha$ ) in the regulation of inflammation in macrophages. *Shock*. 2009;32:62–73.
51. Becker J, Delayre-Orthez C, Frossard N, et al. Regulation of peroxisome proliferator-activated receptor-alpha expression during lung inflammation. *Pulm Pharmacol Ther*. 2008;21:324–330.
52. Miglio G, Rosa AC, Rattazzi L, et al. The subtypes of peroxisome proliferator-activated receptors expressed by human podocytes and their role in decreasing podocyte injury. *Br J Pharmacol*. 2011;162:111–125.
53. Zhou Y, Kong X, Zhao P, et al. Peroxisome proliferator-activated receptor-alpha is renoprotective in doxorubicin-induced glomerular injury. *Kidney Int*. 2011;79:1302–1311.
54. Bruneau S, Nakayama H, Woda CB, et al. DEPTOR regulates vascular endothelial cell activation and proinflammatory and angiogenic responses. *Blood*. 2013;122:1833–1842.
55. Goto K, Kaneko Y, Sato Y, et al. Leptin deficiency down-regulates IL-23 production in glomerular podocytes resulting in an attenuated immune response in nephrotoxic serum nephritis. *Int Immunol*. 2016;28:197–208.
56. Petrovic-Djergovic D, Popovic M, Chittipol S, et al. CXCL10 induces the recruitment of monocyte-derived macrophages into kidney, which aggravate puromycin aminonucleoside nephrosis. *Clin Exp Immunol*. 2015;180:305–315.

57. Benigni G, Dimitrova P, Antonangeli F, et al. CXCR3/CXCL10 axis regulates neutrophil-NK cell cross-talk determining the severity of experimental osteoarthritis. *J Immunol.* 2017;198:2115–2124.
58. Muthuswamy R, Urban J, Lee JJ, et al. Ability of mature dendritic cells to interact with regulatory T cells is imprinted during maturation. *Cancer Res.* 2008;68:5972–5978.
59. Cunard R, Ricote M, DiCampli D, et al. Regulation of cytokine expression by ligands of peroxisome proliferator activated receptors. *J Immunol.* 2002;168:2795–2802.
60. Daynes RA, Jones DC. Emerging roles of PPARs in inflammation and immunity. *Nat Rev Immunol.* 2002;2:748–759.
61. Jakobsen MA, Petersen RK, Kristiansen K, et al. Peroxisome proliferator-activated receptor alpha, delta, gamma1 and gamma2 expressions are present in human monocyte-derived dendritic cells and modulate dendritic cell maturation by addition of subtype-specific ligands. *Scand J Immunol.* 2006;63:330–337.
62. Galli SJ, Borregaard N, Wynn TA. Phenotypic and functional plasticity of cells of innate immunity: macrophages, mast cells and neutrophils. *Nat Immunol.* 2011;12:1035–1044.
63. Lamkanfi M, Dixit VM. Mechanisms and functions of inflammasomes. *Cell.* 2014;157:1013–1022.
64. Stack EC, Wang C, Roman KA, et al. Multiplexed immunohistochemistry, imaging, and quantitation: a review, with an assessment of Tyramide signal amplification, multispectral imaging and multiplex analysis. *Methods.* 2014;70:46–58.
65. Masuda Y, Shimizu A, Mori T, et al. Vascular endothelial growth factor enhances glomerular capillary repair and accelerates resolution of experimentally induced glomerulonephritis. *Am J Pathol.* 2001;159:599–608.
66. Wysocki L, Sato V. "Panning" for lymphocytes: a method for cell selection. *Proc National Acad Sci.* 1978;75:2844–2848.
67. Sakairi T, Abe Y, Jat PS, et al. Cell-cell contact regulates gene expression in CDK4-transformed mouse podocytes. *Am J Physiol Renal Physiol.* 2010;299:F802–F809.
68. Avni D, Goldsmith M, Ernst O, et al. Modulation of TNF $\alpha$ , IL-10 and IL-12p40 levels by a ceramide-1-phosphate analog, PCERA-1, in vivo and ex vivo in primary macrophages. *Immunol Lett.* 2009;123: 1–8.